J Mater Sci (2018) 53:6665–6680

Electronic materials

Cytotoxicity, genotoxicity and uptake detection of folic acid-functionalized green upconversion nanoparticles Y_2O_3/Er^{3+}, Yb^{3+} as biolabels for cancer cells

D. Chávez-García[1,*], K. Juarez-Moreno[2,3,5,*], C. H. Campos[4], E. M. Tejeda[2], J. B. Alderete[4], and G. A. Hirata[2]

[1] Centro de Enseñanza Técnica y Superior, Campus Ensenada. Camino a Microondas Trinidad S/N Km. 1, Moderna Oeste, C.P. 22860 Ensenada, Baja California, Mexico
[2] Center of Nanosciences and Nanotechnology, Autonomus National University of Mexico, Carretera Tijuana-Ensenada. Km. 107, C.P. 22860 Ensenada, Baja California, Mexico
[3] Centro de Nanociencias y Nanotecnología, Universidad Nacional Autónoma de México, Carretera Tijuana-Ensenada. Km. 107, C.P. 22860 Ensenada, Baja California, Mexico
[4] Facultad de Ciencias Químicas, Universidad de Concepción, Edmundo Larenas 129, Concepción, Chile
[5] Departamento de Fisicoquímica, Centro de Nanociencias y Nanotecnología UNAM, Km. 107 Carretera Tijuana-Ensenada, C.P. 22860 Ensenada, Baja California, Mexico

Received: 24 July 2017
Accepted: 18 December 2017
Published online: 31 January 2018

ABSTRACT

Upconversion nanoparticles (UCNPs) have been used as biolabels for cancer cells due to their ability to absorb near-infrared photons and upconvert them into visible radiation. We reported the synthesis of UCNPs Y_2O_3/Yb^{3+}, Er^{3+} (1, 1 mol%), which upon excitation with infrared photons ($\lambda = 980$ nm) emit green color with a maximum peak centered at $\lambda = 550$ nm. UCNPs were functionalized with folic acid (UCNPs-NH_2-FA) and analyzed by transmission electron microscopy, Fourier transform infrared spectroscopy, XRD, DLS and photoluminescence measurements. UCNPs-NH_2-FA had a particle size of 70 ± 10 nm and exhibit a good luminescence spectrum in comparison with bare UCNPs. Cytotoxicity of different concentrations of bare and functionalized UCNPs was measured with the MTT assay in three cancer cell lines: human cervical adenocarcinoma (HeLa) and human breast adenocarcinoma cells (MDA-MB-231 and MCF-7). Some concentrations of bare UCNPs were cytotoxic for cells; however, after been functionalized, UCNPs resulted to be non-cytotoxic. Genotoxicity of bare and functionalized UCNPs was performed by the comet assay, and no DNA damage was found for any concentration. The internalization of UCNPs-NH_2-FA into cancer cells was confirmed by confocal microscopy showing a cytoplasmic fluorescence signal. UCNPs-NH_2-FA were used to detect cancer cells in suspension by flow cytometry, with a specific green fluorescent signal for effective detection of cells. These results confirm that functionalized UCNPs can be used without any cytotoxic or genotoxic effects for bioimaging to detect and visualize cancer cells.

Address correspondence to E-mail: dalia.chavez@cetys.mx; kjuarez@cnyn.unam.mx

https://doi.org/10.1007/s10853-017-1946-0

Introduction

In the field of biomedicine, nanotechnology is providing new tools for imaging and diagnosis through the synthesis and tuning of new nanomaterials with unique physicochemical properties. Among others, luminescence upconversion nanoparticles (UCNPs) have been used as biolabels for cancer detection, cancer therapy, fluorescence imaging, magnetic resonance imaging and drug delivery [1, 2]. UCNPs are generally phosphor nanoparticles with a crystalline matrix doped with lanthanide ions that can absorb near-infrared (NIR) light (980 nm) and upconvert it to visible light [3]. The crystal host lattice receives the lanthanide ions and has a key influence on the upward conversion process. The size of the lattice not only determines the distance between the doping ions but their relative spatial position, coordination number and the type of anions surrounding the dopant. Two important factors must be considered for the selection of the host network: (1) the low energy of the phonons of the lattice and (2) the size of the doping ions that must have a similar size with respect to the crystalline network [4, 5].

In UCNPs, the first ion of Yb^{3+} acts as a sensitizer and absorbs near-infrared radiation energy (NIR) that is further transferred to the second ion (Er^{3+}) also called the activator. After this, UCNPs emit in the visible range the excess of energy as photons [3]. This phenomenon is called energy transfer upconversion (ETU) [6–8]. By tuning the doping percentage of both the sensitizer and activator ions, it is possible to obtain nanomaterials with different emission colors [9]. The advantage of using NIR is that the phototoxicity is reduced compared with UV light, thus allowing to detect them deeper into biological tissues, [10]. This is known as the optical biological window, where the tissues have the minimal light absorption avoiding with this the undesirable photodamage of cells.

UCNPs exhibit several advantages that include their high quantum yield, narrow emission peak, reduced autofluorescence background and improved tissue penetration depth. In contrast with the fading of color in fluorescent proteins and organic dyes commonly used as biolabels, UCNPs exhibit an enhanced photostability [11].

Major challenges for oncology are the efficient and specific delivery of intracellular agents for cancer diagnosis and treatment. Moreover, this is a priority to overcome the systemic toxicological effects of chemotherapy. Therefore, new avenues to label specifically cancer cells are in development. In this sense, the functionalization of nanoparticles with specific biological ligands such as antibodies and ligand receptors is a trend [12]. Among these, folic acid (FA) has been successfully used [13, 14]. FA is a water-soluble vitamin, essential as a cofactor in several body functions, which includes DNA synthesis and repair, cell division and growth, amino acids and protein synthesis, among others [15]. The uptake of FA into the cells is triggered by its binding to folic acid receptor (FR), a glycosyl-phosphatidylinositol-anchored membrane protein [16]. Then, the complex FA-FR is internalized through endocytosis [14]. It is known that among the three isoforms of FR (α, β and γ), FR-α is overexpressed in a wide variety of human cancer cells such as ovary, kidney, lung, mammary gland, brain and endometrium [15, 17]. This overexpression of FA receptors in the membrane of cancer cells makes them an easy target to be detected by nanoparticles functionalized with FA.

Therefore, the aim of this work was to develop UCNPs with excellent luminescent properties by tuning the molar proportions of dopants and co-dopants, combining lanthanide ions Er^{3+} and Yb^{3+} in the host lattice of Y_2O_3. Moreover, to reduce their cytotoxic and genotoxic effects in cells, UCNPs were functionalized with FA. This allows UCNPs to target and labeling cancer cells with an overexpression of FR. Thereby, this process will make FR a suitable coupling site for FA-functionalized UCNPs on tumor cells so they can be used as biolabels for cancer cell imaging [14].

Herein, we present the synthesis by sol–gel method [18] and the physicochemical characterization of UCNPs obtained by X-ray diffraction (XRD), transmission electron microscopy (TEM), dynamic light scattering (DLS) and Fourier transform infrared spectroscopy (FTIR), and also their luminescent properties studied by spectrofluorometry, for bare and functionalized nanoparticles. UCNPs were coated with a thin silica shell and then functionalized with APTES/TEOS to add amine groups that enable the further FA conjugation on their surface. Moreover, cytotoxicity and genotoxicity of bare and functionalized UCNPs were tested on human cervix carcinoma (HeLa) and breast cancer cells MDA-MB-231 and MCF7. Imaging studies obtained by confocal microscopy reveal that the UCNPs were uptaken by

the cancer cells and cytometry assays allows us to detect the binding of UCNPs-NH_2-FA to cancer cells. Thus, UCNPS synthetized in this work can be further used as biolabels to identify cancer cells by imaging or by flow cytometry.

Materials and methods

Sol–gel synthesis

Synthesis of the UCNPs of $Y_2O_3/Er^{3+}/Yb^{3+}$ was made by the sol–gel method (SG) with concentrations of Yb^{3+} (1 mol%) and Er^{3+} (1 mol%) and annealing temperatures of 1200 °C. The description of the methodology was reported previously by us [19]. Briefly, precursors used for this method were: $Y(NO_3)_3$ (Alfa Aesar 99.9965%), $Yb(NO_3)_3$ (Alfa Aesar 99.9%), $Er(NO_3)_3$ (Alfa Aesar 99.9%). The metal precursor was dissolved in HNO_3 (14 mol%) to obtain a homogeneous and transparent solution. Tartaric acid ($C_4H_6O_6$ Aldrich, USA) was dissolved in de-ionized water at a molar ratio of 1:2 for Er^{3+} and Yb^{3+} metal ions. Each individual solution was mixed under constant stirring, and then both solutions were mixed together and stirred for 24 h at room temperature. Thereafter, pH at 5.0 was verified and the mixture was heated under constant stirring at 80 °C for 2 h to produce a denser sol. Subsequently, the sol was heated at 120 °C until a gel was obtained and it was dried to form the xerogel [18]. Finally, the xerogel was collected and annealed at 1200 °C for 2 h [19]. To avoid agglomeration, UCNPs were ultrasonicated before their analysis by TEM or functionalization. Ultrasonication was done with a high-intensity ultrasonic processor (Sonics & Materials, Inc.) at 70% of the amplitude for about 30 min with 20 ml of isopropanol/ethanol.

Silica and aminosilane functionalization

The amino groups added on the surface of the UCNPs through the 3-aminopropyl-trimethoxysilane (APTES) functionalization, allowed the binding of FA to them. Silica-coating and aminosilane functionalization were made by the APTES/TEOS technique [9]. Firstly, a Stöber synthesis methodology was used to coat the UCNPs with a thin silica shell [20]. Briefly, a solution of 10 mmol of UCNPs was stirred for 20 min. In parallel, another solution containing pure ethanol and 0.6 ml of tetraethyl orthosilicate, TEOS, (Sigma-Aldrich, MO, USA) was prepared. Both solutions were added to a previously mixed solution containing 1 ml of ammonium hydroxide (NH_4OH, Sigma-Aldrich, MO, USA), 0.2 ml of IGEPAL surfactant (Sigma-Aldrich, MO, USA) and 9 ml of distilled water and were constantly stirred for 24 h. Then, the silica-coated UCNPs were centrifuged three times at 2000 rpm for 15 min at 24°C. Finally, silica-coated UCNPs were filtered and then annealed at 900 °C for 2 h as previously reported [21].

Silica-coated UCNPs were ultrasonicated for 15 min before aminosilane functionalization. Afterward, silica-coated UCNPs were mixed for 4 h in a solution of ethanol containing 0.02 ml of APTES (98%, Sigma-Aldrich), 0.14 ml of TEOS and 0.2 ml of ammonium hydroxide. After this, the aminosilane-functionalized UCNPs (UCNPs-NH_2) were air-dried and collected [9].

Folic acid conjugation to UCNPs

The amino groups added by APTES/TEOS functionalization to the UCNPs (UCNPs-NH_2), enable a further FA conjugation. In this context, the UCNPs-NH_2 were functionalized with FA ligands to bind to FR expressed on the membrane of cancer cells. Functionalization reaction of UCNPs-NH_2 with FA was done with a Schlenk system in a N_2 atmosphere. Firstly, 0.500 g of FA (Sigma-Aldrich, MO, USA) and 500 µl of triethylamine (TEA, Sigma-Aldrich, MO, USA) were added in 10 ml of dry dimethyl sulfoxide (DMSO, Sigma-Aldrich, MO, USA) where the mixture was agitated for 2 h at 37 °C. Then, 0.260 g of *N*-hydroxysuccinimide (NHS, 99% Sigma-Aldrich, MO, USA) and 0.470 g of *N*,*N*′-dicyclohexylcarbodiimide (DCC, 99% Sigma-Aldrich, MO, USA) were added to the solution and stirred at 37 °C in darkness for 12 h to obtain FA-NHS. After this, the mixture was filtered through a pore diameter of 0.22 µm to separate the by-products. UCNPs-NH_2 were dispersed in 25 ml of a carbonate/bicarbonate buffer (0.01 M, pH 9.0) and ultrasonicated for 5 min. Then, 3 ml of FA-NHS solution were added to the UCNPs-NH_2. After this, UCNPs-NH_2 were agitated in darkness for 2 h. The resulted UCNPs-NH_2 functionalized with FA (UCNP-NH_2-FA) were centrifuged at 6000 rpm for 15 min, washed three times with 45 ml of DMSO followed by five rinses with 45 ml of ethanol. Finally, UCNPs-NH_2-FA were vacuum-dried overnight at 30 °C. The final material turned into a powder of

yellow color. The modification rate was measured by UV–Vis follow the activated-FA consumption during the conjugation with the UCNPs-NH_2.

Characterization of UCNPs

Crystallinity of bare UCNPs was characterized by X-ray diffraction analysis (XRD) with a Phillips X'Pert-MPD diffractometer equipped with Cu Kα radiation ($\lambda = 0.15406$ nm). Measurements scanned over 2θ range of 10°–80° were taken with a step size of 0.1° and a 1 s dwell per point. The results obtained were compared with the database PCPDFWIN as previously reported [19]. The morphology and nanoparticle size of UCNPs were assayed by transmission electron microscopy (TEM) using a JEOL JEM-2100-F microscope. Moreover, the presence of the silica covering was confirmed by energy-dispersive spectrometry (EDS) technique. Average size of nanoparticle and Zeta potential were measured by dynamic light scattering (DLS) with a Zetasizer Nano ZS instrument (Malvern). The photoluminescence of the UCNPs was analyzed with a fluorescence spectrometer with dried UCNPs (PL, Hitachi® FL-4500) with 980 nm for excitation. For the determination of external quantum efficiency, we used the method introduced by De Mello et al. [22]. The calculations were aided by means of a 60-mm integrating sphere, a CCD (InstaSpec IV), and an Oriel® MS260i™ high-resolution 1/4 m imaging spectrograph.

To confirm the folic acid functionalization on UCNPs surface, Fourier transform infrared spectroscopy analysis (FTIR) was done in the range of 400–4000 cm^{-1} (Thermonicolet 1700).

Cell culture

Human epithelioid cervix carcinoma HeLa cells (CCL-2) and human breast cancer cells MDA-MB-231 (CRM-HTB-26) and MCF7 (HTB-22) were obtained from American Type Culture Collection (ATCC, Manassas, Virginia, USA). Cancer cell lines were cultivated according the supplier directions. HeLa and MDA-MB-231 cells were cultivated in RPMI-1640 media (Sigma-Aldrich, MO, USA) supplemented with 10% Fetal Bovine Serum (FBS, BenchMark, Gemini Bio Products), 1% penicillin–streptomycin (Sigma-Aldrich, MO, USA), 1% L-glutamine (Sigma-Aldrich, MO, USA) and 1.5 g/l sodium bicarbonate. Human breast cancer cells MCF7 were cultured in Dubelcco's Modified Eagle's medium (DMEM, Sigma-Aldrich, MO, USA) supplemented with 10% SFB, 1% penicillin–streptomycin, 1% L-glutamine, 1.5 g/l sodium bicarbonate and 0.01 mg/ml of human recombinant insulin (Sigma-Aldrich, MO, USA). Cells were propagated in growth medium and maintained at 37 °C with 5% CO_2.

Cytotoxicity assay

Cell viability was assessed by the method described by Mosmann [23], using a colorimetric assay based on the reduction of 3-(4,5-dimethyl-2-thiazolul)-2,5-diphenyl-2H-tatrazolium bromide (MTT) to water-insoluble blue formazan crystals by the mitochondrial dehydrogenase enzymes. Cytotoxicity of both bare and functionalized UCNPs (UCNPs-NH_2-FA) was tested on HeLa, MDA-MB-231 and MCF-7 cancer cell lines. UCNPs dilutions were performed in DMEM media without supplements. Cells were exposed to different concentrations of UCNPs from 0.001 to 1 μg/ml for 24 h in a 96-well plate containing 10,000 cells per well. Treated cells with UCNPs were incubated at 37 °C and 5% CO_2 atmosphere. After incubation time, cells were washed three times with phosphate buffer solution, PBS (137 mM NaCl, 2.7 mM KCl, 10 mM Na_2HPO_4, 1.8 mM KH_2PO_4 pH 7.4) and cell viability test was assessed with the in vitro toxicology assay kit TOX-1 (Sigma-Aldrich). DMSO was used to induce total cell death, while cell growth under ideal conditions was assayed with the incubation of cancer cells in DMEM media without UCNPs. Absorbance measurements with an ELISA plate reader (Thermo Scientific, USA) at 570 and 690 nm, allowed the comparison of cell viability between control groups and the damage induced by different concentrations of UCNPs on cells. The background absorbance of cell viability test was performed by measuring the absorbance of multiwell plates at 690 nm and subtracts it from the absorbance values obtained at 570 nm. All data obtained from UCNPs-treated cells were normalized to data from three positive control wells with no treatment in three independent experiments with their internal triplicates.

Alkaline single-cell gel electrophoresis (comet assay)

To evaluate whether the incubation of solutions with different concentrations of UCNPs with cancer cell lines could induce DNA damage (i.e., single and

double breaks in DNA), an alkaline single-cell gel electrophoresis assay or comet assay was performed as described previously by Singh et al. [24].

Cancer cells HeLa, MDA-MB-231 and MCF7 were incubated with different concentrations of UCNPs from 0.001 to 1 μg/ml for 24 h at 37 °C and 5% CO_2 atmosphere. Cells were incubated under the same conditions without UCNPs as negative control. Afterward, cells were washed and collected in PBS, to embedded in 0.5% low melting point agarose on comet slides. The slides were covered with a cover glass and kept at 4 °C to create a microgel. Each slide was immersed for 1 h in pre-chilled lysis solution containing 2.5 M NaCl, 100 mM Na_2EDTA and 10 mM tris-base, at pH 10 with 1% Triton X-100 and 10% DMSO. Samples were subjected to denaturation in alkaline buffer (0.3 M NaCl, 1 mM EDTA) for 20 min in darkness. Electrophoresis was performed at 25 V and 300 mA for 20 min. Slides were immersed in a cold neutralizing buffer (0.4 M tris-hydrochloric acid, pH 7.5) for 15 min and then, dehydrated by incubation in 99% ethanol for 5 min. The slides were air-dried and stained with a solution of ethidium bromide (at 1 mg/mL) in dark. Sample slides were visualized with an Axio Lab A1 epifluorescence microscope equipped with an excitation filter of 365 nm and barrier filter of 455 nm connected to a digital camera (Axio Cam ICc5.D). A single analyst performed the visual scoring of slides to minimize scoring images variation. Analysis was done using the free-software ImageJ developed by the National Institutes of Science (NIH). Data were based on the analysis of 200 comets for each test visually scored. Comets were classified visually to belong into one of the five classes according to tail size. Class o were scored for undamaged cells showed as intact nuclei without tails, whereas damaged cells showed the appearance of a comet score as follows: 0 = no damage; 1 = low damage; 2 = medium damage and 3 = high damage. The DNA damage index is based on the length of migration and on the amount of DNA in the tail and is given by the formula: DNA damage index: $[(0 \times n_0) + (1 \times n_1) + (2 \times n_2) + (3 \times n_3)]$, where n is the total amount of counts for each class [25].

Confocal microscopy cell imaging

Cell culture Petri dishes coated with Poly-D-lysine (MatTek Co. MA, USA) were used to seed 300,000 cancer cells in cell culture media and incubated overnight at 37 °C with 5% CO_2. Then, HeLa, MDA-MB-231 and MCF7 cells were incubated with 1 μg/ml of UCNPs for 24 h at 37 °C under 5% CO_2 atmosphere. After this, cells were rinsed with PBS and then fixed with 4% formaldehyde in PBS solution at 4 °C for 15 min. After fixation, cells were permeabilized with 0.5% Triton X-100 in PBS for 15 min at 4 °C. Nuclear staining was achieved by incubated the cells with 4′, 6-diamidino-2-phenylindole (DAPI) at 0.5 ng/μl in darkness for 10 min at 24 °C, followed by eight washes with PBS.

Images of cells were obtained with an inverted laser scanning microscope Olympus FluoView FV1000 (Japan). Nuclear staining with DAPI was visualized using an argon ion laser for excitation at 405 nm with DAPI filters for emission at 455 nm. Luminescence of UCNPs was detected using the NIR laser (980 nm) and EGFP filter channel (excitation at 488 nm and emission at 515–530 nm). A Plan Achromatic 60x/1.48 N.A. oil immersion objective was used. A photomultiplier module allows the simultaneous view of the fluorescence in the entire cell. Laser intensity was kept at 20% to reduce photobleaching. The imaging parameters used produced no detectable background signal from any source other than from UCNPs and DAPI. Confocal images were captured using the FV-10 ASW software and were analyzed with the FV-10ASW viewer version 4.1 from Olympus [26].

Detection of cancer cells with UCNPs by flow cytometry

HeLa, MDA-MB-231 and MCF7 cancer cells (4×10^5) were incubated with 1 μg/ml of UCNPs for 24 h at 37 °C under 5% CO_2 atmosphere. After this, cells were rinsed with PBS and harvested with Trypsin/EDTA (Sigma-Aldrich, MO, USA). Then, cells were centrifuged at 1200 rpm for 5 min, rinsed twice with PBS, and finally cell pellet was resuspended in 1 ml of PBS and further analyzed by flow cytometry using an Attune NxT flow cytometer (Life Technologies, Carlsbad, CA, USA). Recorded data from flow cytometry consist of 30,000 events (cells) analyzed with the BL1 channel. Flow cytometry analysis was

performed with the Attune NxT software (life Technologies).

Statistical analysis

With exception of confocal imaging acquisition, all other experiments were done in a threefold-independent manner with internal triplicates. The results were expressed as mean ± standard deviation of three independent experiments. Data were evaluated by analysis of variance (ANOVA), followed by Tukey's multiple comparison test, using Graph Pad Prism 6.0 software. The results were considered statistically significant when $p < 0.05$.

Results

XRD and TEM images of Y_2O_3/Er^{3+}, Yb^{3+} UCNPs

The composition obtained for the UCNPs synthesized was $(Y_{0.98}Yb_{0.1}Er_{0.1})_2O_3$. The XRD patterns of the UCNPs are showed in Fig. 1a. All the diffraction peaks are consistent with the JCPDS No. 89-5592 (Y_2O_3) database (blue). XRD result of the sample is showed in green color and all the characteristic diffraction peeks (211), (222), (400), (440) and (622) were present, confirming the cubic structure of the sample.

The TEM images of both bare and FA-functionalized UCNPs $Y_2O_3/Er^{3+}/Yb^{3+}$ (1, 1%) obtained by sol–gel are shown in Fig. 1b, c. The morphology of UCNPs $Y_2O_3/Er^{3+}/Yb^{3+}$ obtained was mostly spheroidal, whereas their average diameter obtained by DLS was 70 ± 10 nm. As observed in Fig. 1c, the silica shell of UCNPs-NH_2-FA is shown to be approximately of 5 nm thick. As observed in Fig. 1c, UCNPs tend to agglomerate after functionalization and during the preparation of the sample for TEM. However, after APTES/TEOS and FA functionalization, UCNPs do not agglomerate.

Upconversion luminescence of nanoparticles and external quantum efficiency

Upconversion luminescence spectra of bare and functionalized UCNPs-NH_2-FA, under 980 nm laser excitation, are shown in Fig. 2. The emission of the

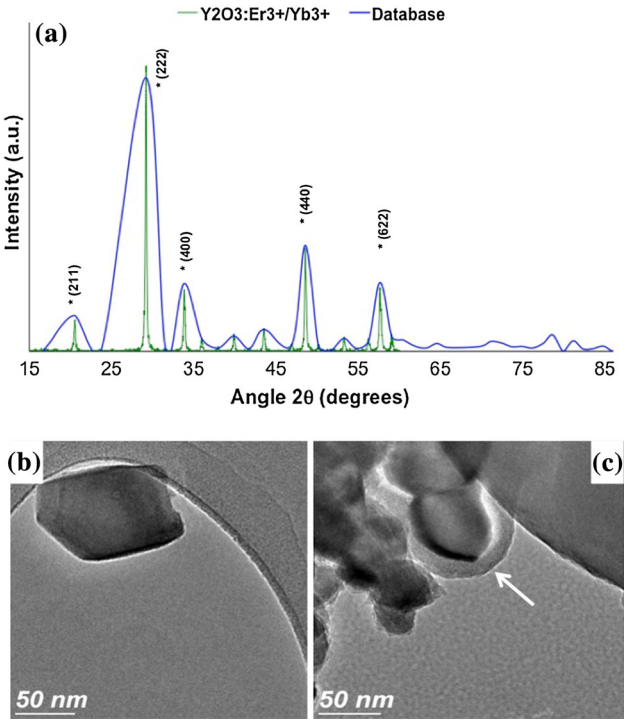

Figure 1 XRD and TEM images of Y_2O_3/Er^{3+}, Yb^{3+} UCNPs. **a** Comparison of XRD patterns of JCPDS No. 89-5592 (Y_2O_3) database (blue line) and $Y_2O_3/Er^{3+}/Yb^{3+}$ (1, 1 mol%) (green line). Representative TEM images of **b** bare UCNPs $Y_2O_3/Er^{3+}/Yb^{3+}$ (1, 1 mol%) and **c** functionalized UCNPs-NH_2-FA.

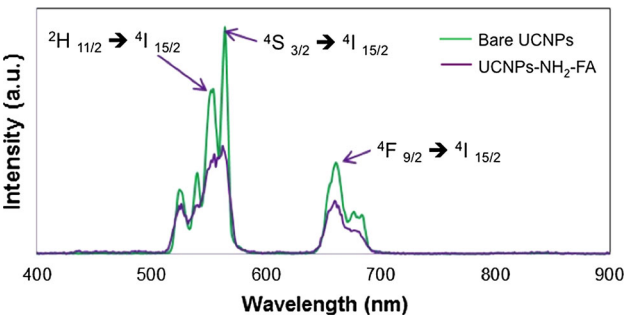

Figure 2 Upconversion emission spectra under 980 nm excitation for bare UCNPs (purple line) and UCNPs doped with Er^{3+}/Yb^{3+} (1, 1 mol%) and functionalized with aminosilane-folic acid (green line). All the samples measured were dried powder.

nanoparticles Y_2O_3/Er^{3+}, Yb^{3+} (1, 1 mol%) was in green at 564 nm. In Fig. 2, it is also showed the electronic transitions present in the spectra were $^2H_{11/2} \rightarrow {}^4I_{15/2}$ (550 nm), $^4S_{3/2} \rightarrow {}^4I_{15/2}$ (564 nm) and $^4F_{9/2} \rightarrow {}^4I_{15/2}$ (660 nm).

Calculations for external quantum efficiency on bare UCNPs result in a value of 1.15% ± 0.11%. Analysis for UCNPs-NH_2-FA gives a value of 0.01%.

A calculated value of 8.9% absorption (for $\lambda_{exc} = 974$ nm) for UCNPs-NH_2-FA contrasts with 1.9% calculated for bare UCNPs. However, bare UCNPs were less absorbent but six times more intense in its PL emission than functionalized UCNPs-NH_2-FA suggests that the outer layers are responsible for most of the near-infrared pumping excitation absorption.

EDS spectra of coated UCNPs

Energy-dispersive X-ray spectroscopy (EDS) is an analytical technique used for the elemental analysis or chemical characterization of a sample. It relies on the interaction of some source of X-ray excitation in a given sample. Its characterization capabilities are due in large part to the fundamental principle that each element has a unique atomic structure rendering a unique set of peaks on its X-ray emission spectrum. In this context, the EDS technique was used to verify the elements contained on the UCNPs and to confirm whether the silicon coating was present on their surface. The spectrum is shown in Fig. 3.

FTIR analysis of UCNPs

To verify the functionalization of UCNPs with amine and FA groups, a Fourier transform infrared spectroscopy analysis (FTIR) was used. FTIR is a technique that simultaneously collects high spectral resolution data over a wide spectral range; it is used to obtain an infrared spectrum of absorption or emission of a specific sample.

The presence of the aminosilane groups and FA on the surface of functionalized UCNPs was confirmed by FTIR, as showed in Fig. 4. FTIR spectrum of bare UCNPs is shown in Fig. 4 with blue line, for reference. Also Fig. 4 shows the FTIR spectrum of aminosilane-functionalized UCNPs (red line), where it shows the presence of the amino groups: wagging of NH_2 at 669–793 cm^{-1}, primary amines at 1541 cm^{-1} and secondary amines at 3341 cm^{-1}.

The FA-functionalized UNCPs (UCNPs-NH_2-FA) are shown with black line, which confirms that the UCNPs are functionalized with FA, since the vibration of FA ligands at 3375, 3124 and 2960 cm^{-1} and the FA –NH_2 groups at 1659, 1606 and 1512 cm^{-1} are observed.

Zeta potential measurement by DLS analysis of UCNPs

The stability of UCNPs was measured through the Zeta potential. It is evident that the Zeta potential of functionalized nanoparticles (UCNPs-NH_2-FA) did not change significantly with their storage. Interesting is that after being functionalized either with APTES/TEOS or with FA, nanoparticles tend to be more stable than the bare UCNPs as it can be

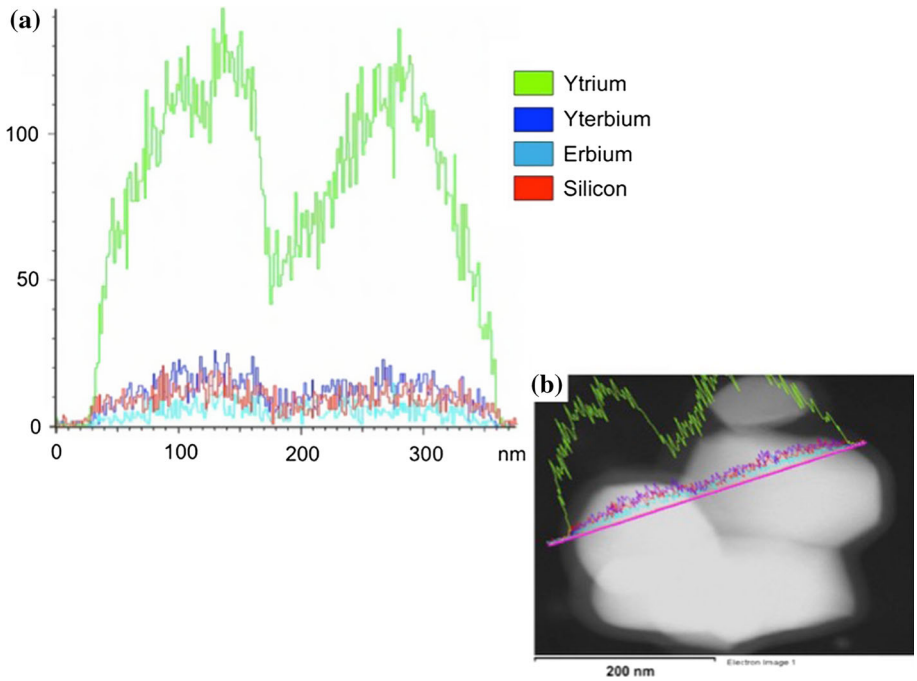

Figure 3 **a** EDS spectra of silica-coated UNCPs Y_2O_3/Er^{3+}/Yb^{3+} (1, 1 mol%). In **b** it is showed the elements present on the surface of silica-coated UCNPs.

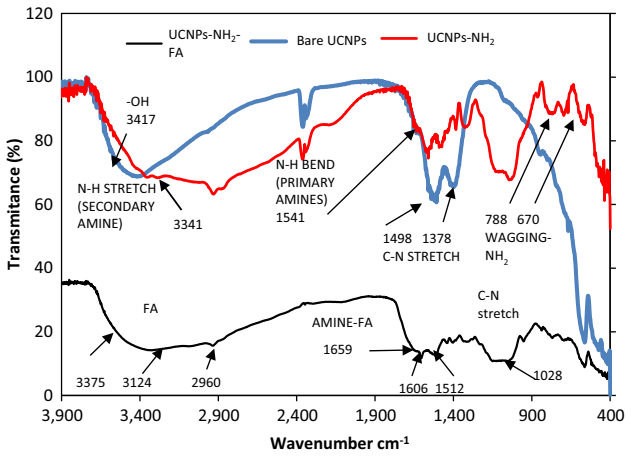

Figure 4 FTIR spectra of, bare UCNPs $Y_2O_3/Er^{3+}/Yb^{3+}$ (1, 1 mol%) (blue line), UCNPs with aminosilane functionalization (red line) and functionalized UCNPs-NH_2-FA (black line).

observed by their Zeta potential values in Fig. 5a. As showed in Fig. 5b, comparison of Zeta potential measurements of nanoparticles at day 0 and after 15 days of being stored in distilled water at 4 °C was achieved.

Cytotoxicity assay of UCNPs in cancer cell lines

The cytotoxicity effect of bare and functionalized UCNPs-NH_2-FA incubated with cervix (HeLa) and breast cancer cells (MDA-MB-231 and MCF7) are shown in Fig. 6. The lower concentrations of bare UCNPs (0.001 μg/ml) showed less cell viability than higher concentrations (0.1 μg/ml). This is explained due to the agglomeration and precipitation tendency exhibited by bare UCNPs, thus interfering with the absorbance reading measurements of the plate. However, after FA functionalization, the agglomeration tendency of UCNPs was reduced. The cytotoxicity effect of UCNPs in human cervix and breast cancer cell lines was diminished after been functionalized with aminosilane and FA groups (UCNPs-NH_2-FA), as showed in Fig. 6a for HeLa cells and Fig. 6b, c for breast cancer cells MCF7 and MDA-MB-231. Taking these results in consideration, we test whether UCNPs-NH_2-FA were able to be use as biolabels for cancer cells as it is shown in the next section.

Genotoxicity of bare and functionalized UCNPs-NH_2-FA

Genotoxicity is a key parameter when evaluating the toxicity of a given nanomaterial. This can be determined by the DNA damage using different approaches such as alkaline single-cell gel electrophoresis or comet assay. With this method it is possible to evaluate single- and double-strand fragmentations in DNA. In this study, human cervix adenocarcinoma (HeLa) and breast cancer cells (MDA-MB-231 and

(a)

Nanoparticle	Zeta potential (mV) Average ± SD
Bare UCNPs	25.1 ± 4.59
UCNPs-NH_2-	-14.7 ± 3.80
UCNPs-NH_2-FA (day 0)	-11.8 ± 4.30
UCNPs-NH_2-FA (day 15)	-14.6 ± 4.06

(b)

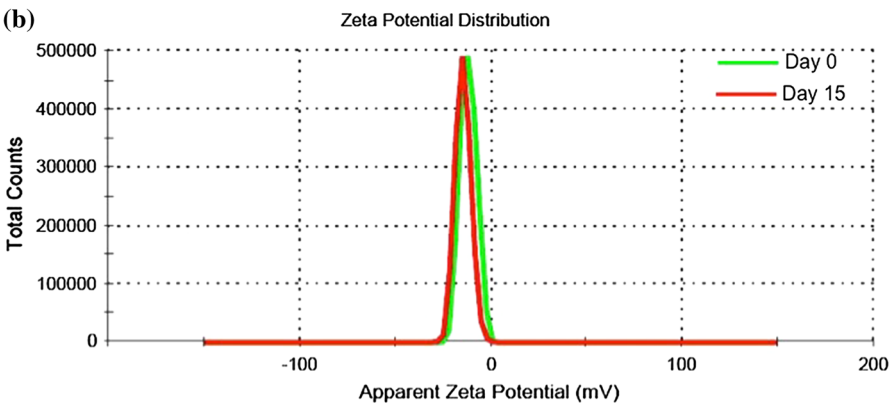

Figure 5 Zeta potential of bare and functionalized UCNPs. **a** Comparison of Zeta potential obtained in each step of the synthesis protocol, bare and functionalized nanoparticles. **b** Comparison of Zeta potential between UCNPs-NH_2-FA at day 0 and after 15 days of being stored in distilled water at 4 °C.

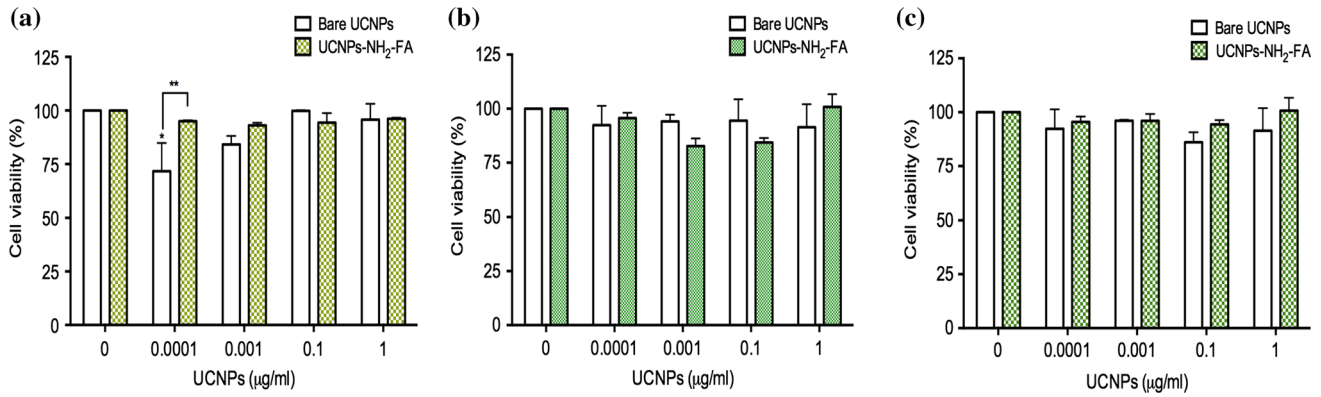

Figure 6 Cell viability assay of bare UCNPs $Y_2O_3/Er^{3+}/Yb^{3+}$ (1, 1%) (white bars) and functionalized UCNPs-NH_2-FA (green color bars) in **a** human epitheloid cervix carcinoma HeLa cells and **b** human breast cancer cell line MCF7 and **c** MDA-MB-231. Cell viability test is based on the reduction of MTT reagent. Results represent the mean ± standard deviation of three independent experiments * $p < 0.05$; ** $p < 0.01$ and *** $p < 0.001$.

MCF-7) were exposed to bare UCNPs and functionalized UCNPs-NH_2-FA at different concentrations for 24 h. The scores of DNA damaged for the three types of cancer cells are shown in Fig. 7.

As observed in Fig. 7a, the DNA damage index for HeLa cells treated with 0.001–1 μg/ml of bare and functionalized UCNPs was similar to those values obtained for untreated cells ($p > 0.05$). The same results were observed for both cancer cell lines MDA-MB-231 and MCF7, as observed in Fig. 7b, c. Thus, when comparing the DNA damage index of control cells (without treatment) with those obtained in the exposed cells to UCNPs, no difference was found. Therefore, no genotoxic effect was induced for the exposure of cancer cells to UCNPs. This parameter is important when assessing an efficient biolabel for imaging detection.

Cancer cell imaging with UCNPs

In this study, we took advantage of the overexpression of FA receptors on the cell membrane of cancer cells. Thus, UCNPs-NH_2-FA used herein were used to bind to this FA receptors presented in both, cervix adenocarcinoma (HeLa) and breast cancer (MB-MDA-231 and MCF7) cells. To corroborate this, images of UCNPs-NH_2-FA internalized into cancer cells were obtained by confocal microscopy as it is shown in Fig. 8.

Confocal images of nucleus (*n*) stained with DAPI are showed in Fig. 8. UCNPs-NH_2-FA were internalized into HeLa, MDA-MB-231 and MCF7 cells. Localization of UCNPs-NH_2-FA was detected in the cytoplasmic region of all cancer cells (white arrows); this was possible due to the green emission light of UCNPs-NH_2-FA excited with NIR 980 nm. Merge of the images allows the visualization of both nuclear staining and internalized UCNPs-NH_2-FA, as expected they were clearly localized in the cytoplasmic region, since FA ligands were used for UCNPs internalization.

Functionalized UCNPs $Y_2O_3/Er^{3+}/Yb^{3+}$ (1, 1 mol%) were incubated with human cervix adenocarcinoma HeLa cells and breast cancer cell lines MDA-MB-231 and MCF7 for 24 h. Nuclear staining with DAPI is labeled as "*n*." Detection of functionalized UCNPs-NH_2-FA in the cytoplasm of cancer cells is shown with white arrows. Merge of DAPI and green emission of UCNPs-NH_2-FA in the cytoplasm of cancer cells is presented, where nucleus and nanoparticles are labeled as previously indicated. Scale bar represents 30 μm.

Cancer cells detection with UCNPs-NH_2-FA by flow cytometry

Considering that both cervical and breast cancer cell lines were able to uptake FA-functionalized UCNPs. We test whether the detection of these cancer cells in suspension was possible by flow cytometry. For this, human cervical HeLa cancer and breast cancer (MDA-MB-231 and MCF7) cell lines were incubated with 1 μg/ml of either bare or functionalized UCNPs. As it is shown in Fig. 9a, c, e, bare UCNPs were not able to bind to any of the cancer cell lines here used. However, an increase in the fluorescence intensity

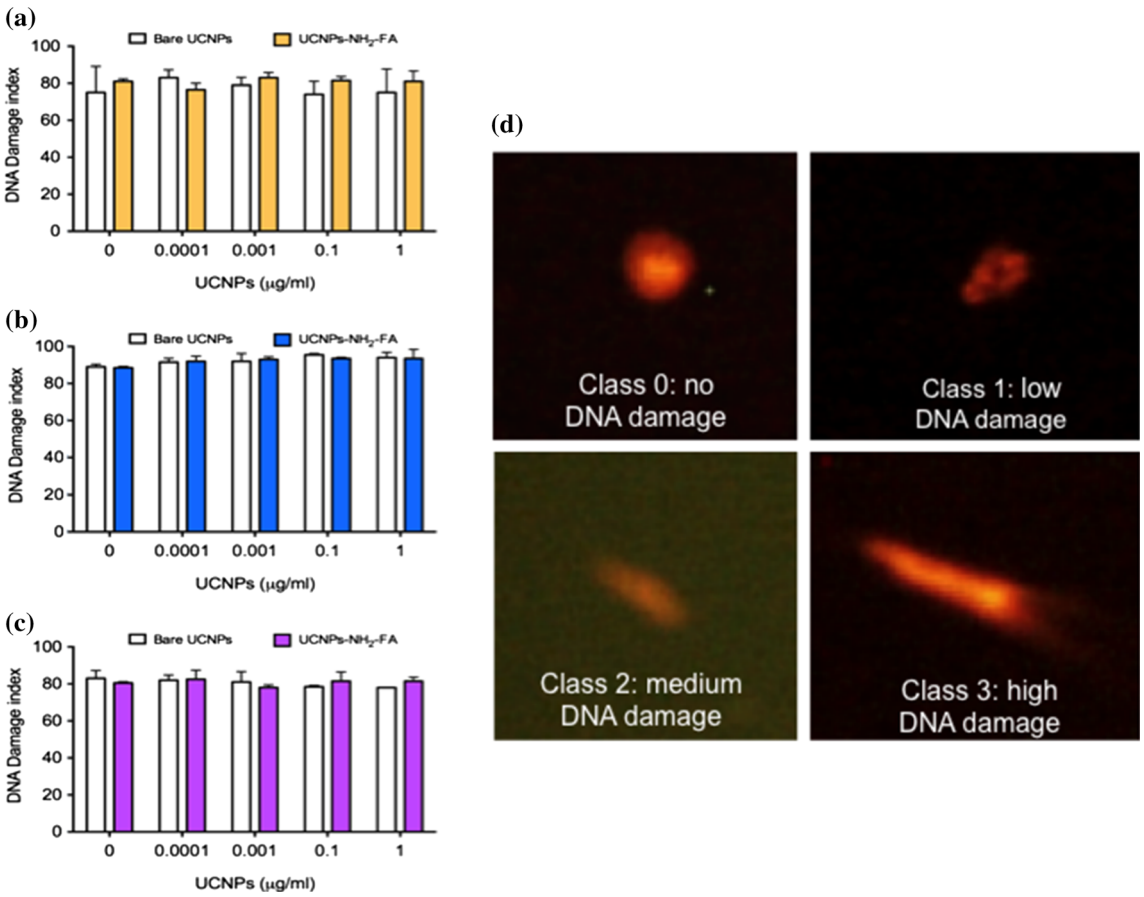

Figure 7 Genotoxicity assay of bare UCNPs $Y_2O_3/Er^{3+}/Yb^{3+}$ (1, 1%) (white bars) and functionalized UCNPs-NH_2-FA (color bars) on HeLa, MDA-MB-231 and MCF7 cancer cells. DNA damage index of **a** HeLa, **b** MDA-MB-231 and **c** MCF7 cells exposed to UCNPs at different concentrations was assessed by comet assay. **d** DNA damage categorization by comet assay according to tail size. Non-treated cells were incubated with cells culture media to simulate normal conditions and taken as the negative control group. Data represent the mean ± standard deviation of three independent experiments. Statistical analysis by ANOVA and Tukey's multiple comparison revealed no significance (ns).

was clearly detected when UCNPs-NH_2-FA were added to the cancer cells, as depicted in Fig. 9b, d, f. With these results, we confirm that UCNPs-NH_2-FA can be used as cancer cell biolabels. Moreover, this emphasizes that besides the advantages of their physicochemical properties, UCNPs have probe to be safe in terms of cytotoxicity and genotoxicity. This makes the UCNPs herein used excellent biolabels nanotools for cancer cell detection either by imaging or by flow cytometry.

Discussion

Nanomaterials based on lanthanide ions exhibit both downconversion (conventional Stokes type) and upconversion (anti-Stokes) luminescence [6]. In this sense, UCNPs have a long luminescence lifetime and are characterized for their capability to absorb NIR light and upconvert it to visible light [27]. Additionally, the composition of their sensitizer ions can be tuned to obtain certain type of emissions that have been applied for biomedical applications. For example, in this study we synthesized UCNPs with 1% molar concentrations of Er^{3+}, Yb^{3+} ions, which resulted to show the characteristic green emission of the electronic transitions $^2H_{11/2} \rightarrow {}^4I_{15/2}$ (550 nm) and $^4S_{3/2} \rightarrow {}^4I_{15/2}$ (564 nm) and exhibited a cubic structure verified by a detailed in the XRD and PL analysis. If the percentage of the Yb^{3+} ion is increased, the transition $^4F_{9/2} \rightarrow {}^4I_{15/2}$ (660 nm) is present with more intensity and the color of emission will change to red, more detailed information about this process is shown on our previous paper [19].

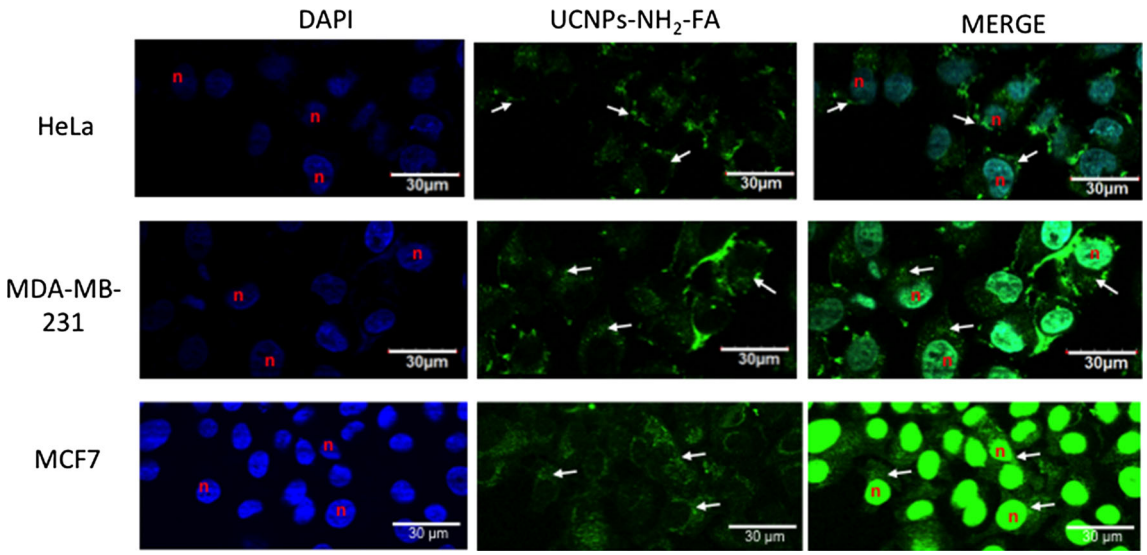

Figure 8 Cellular localization of fluorescence green emission UCNPs-NH_2-FA.

Figure S1 exhibits the electronic transitions between the Yb^{3+} and Er^{3+} ions for the upconversion process, showing with red arrow the red emission and the green emission with green arrow [6].

Contrary to other luminescent particles, UCNPs do not bleach due to their chemical stability [28]. The photoluminescence of bare and functionalized UCNPs-NH_2-FA showed that although functionalized UCNPs had less intensity as the bare nanoparticles, both UCNPs showed good emission spectra with a green emission at 564 nm. The advantage of this type of UCNPs is that their excitation energy is NIR light, which is safer to the body and can penetrate tissue as deep as several inches [29]. Bare UCNPs being less absorbent but more intense in its PL emission than functionalized UCNPs-NH_2-FA suggests that the outer layers are responsible for most of the absorption from the near-infrared pumping excitation. Even though, the functionalized UCNPs were clearly located into cell cytoplasm, showing that the diminished luminescence is good for cell identification.

Taking these in consideration, in this work we synthesized UCNPs with a crystal host of Y_2O_3, doped with the same molar concentrations (1%) of both ions Er^{3+} and Yb^{3+}, which allows us to obtain UCNPs with an intense green emission particularly useful for cancer cells biolabeling.

To be useful for biological assays, UCNPs must be dispersible in aqueous solution and be covered with biological ligands to increase their selectivity and targeting. The UCNPs synthetized in this work were coated with a 5-nm-thick silica shell; however, they tend to agglomerate after and during coating. To overcome this, we decided to use the IGEPAL surfactant along with the APTES/TEOS covering technique. This resulted in a homogeneous coating on all UCNPs and also added silane groups in the surface of the nanoparticles. The silanization is a powerful technique used for covalent modification of surface nanoparticles, among others of silica surface, this can be further used to covalent binding of biological ligands such as FA [30].

It is well known that some types of cancer cells such as breast, ovary and lung overexpress the FA receptors in their cell membrane [14, 17, 31]. Also, FA ligands have a high binding affinity to FA receptors, which are overexpressed on the surface of cervical adenocarcinoma (HeLa) and breast cancer cells such as MDA-MB-231 and MCF7 [2, 32]. Thus, to specifically site direct the UCNPs here studied to cancer cells, a FA ligand was linked to their surface through the silane group. This was confirmed by FTIR, which showed the presence of characteristic peaks corresponding to vibration of amine-folic acid bonds on the surface of the UCNPs. It has been reported that when FA was chemically linked with amine or c-carboxyl groups, its FA receptor binding affinity increased [32–34] enhanced with this the capability of UCNPs functionalized with FA to bind to FR located at the surface of cancer cells.

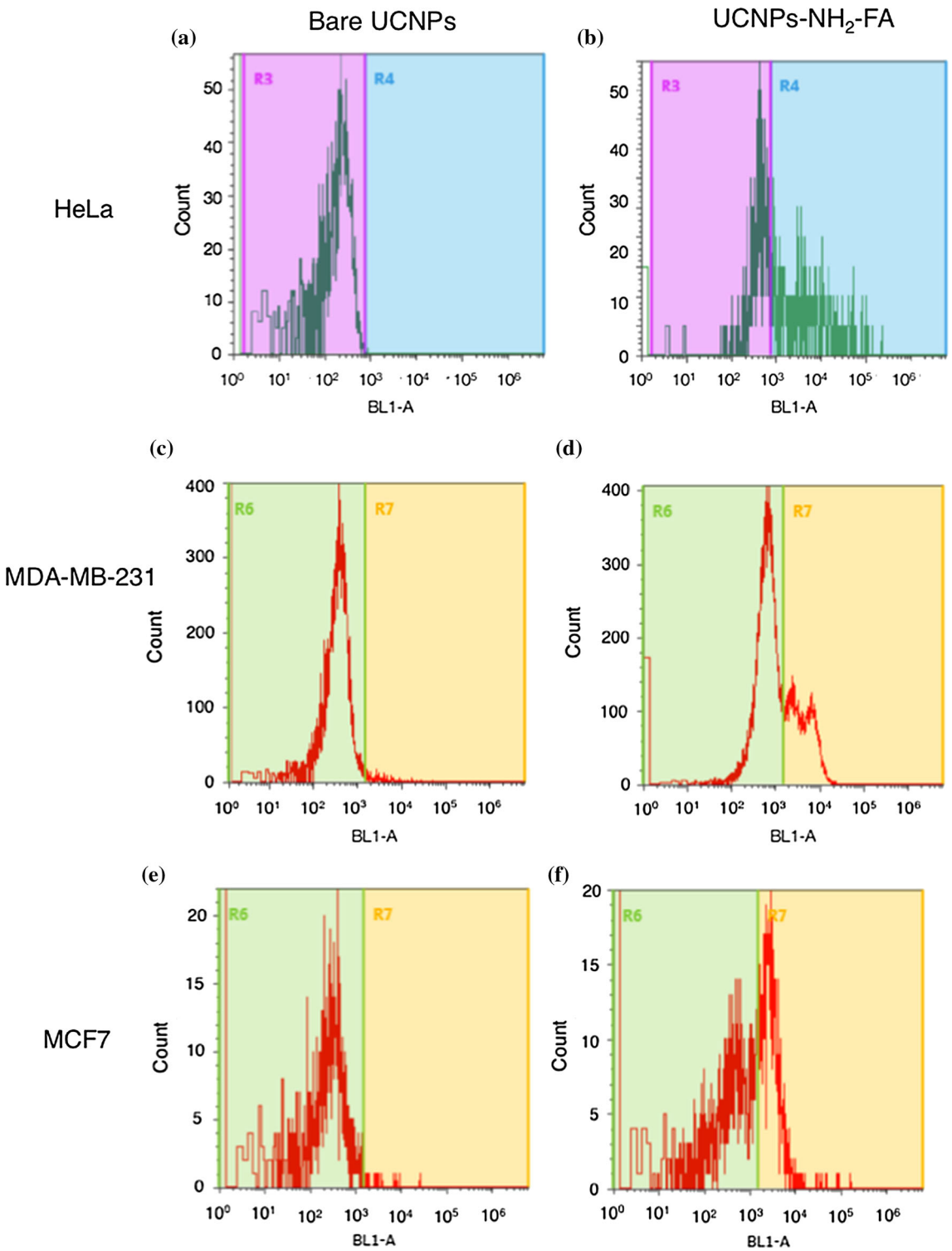

Figure 9 Flow cytometry detection of cancer cells with functionalized UCNPs-NH_2-FA. Human cervical adenocarcinoma (HeLa) cells and human breast MDA-MB-231 and MCF7 cancer cells incubated with bare UCNPs (**a**, **c**, **e**) and functionalized UCNPs-NH_2-FA (**b**, **d**, **f**). Green emission of UCNPs was detected with the BL1-channel.

When assessing the toxicity of a given nanomaterial, cell viability tests are fundamental to provide information related with cell survival, metabolic status and cell death modality of treated cells. If this nanomaterial is intended to be used as a cell biolabel, it must fulfill several criteria including

biocompatibility and toxicological assessment to assure that its binding to the target cell will not damage it either by leading to cell death or by causing any genotoxic effect [9]. Thereby, besides their physicochemical characterization, biological characterization of UCNPs must include the evaluation of their cytotoxic and genotoxic effects in cancer cells.

Cytotoxicity is used to test if a reagent affects the viability of a given cell population and causes cellular damage that leads to cell death. In this case, we used a colorimetric assay based on the reduction of MTT into formazan, this transformation reflects the metabolic status of a cell population after being exposed to the UCNPs here evaluated.

To evaluate whether the functionalization with aminosilane-folic acid (NH_2-FA) on the surface of UCNPs caused any cytotoxic effect on cancer cells, cell viability tests were carried out on three different cancer cell lines (HeLa, MDA-MB-231 and MCF7). The results revealed that the three cancer cell lines exhibited a differential susceptibility to bare UCNPs composed of $Y_2O_3/Er^{3+}/Yb^{3+}$ (1, 1%) and functionalized UCNPs-NH_2-FA. For example, HeLa and MCF7 cell lines resulted to be more sensitive to bare UCNPs than MDA-MB-231 breast cancer cells. However, after functionalization with aminosilanes and FA groups, the cytotoxicity of UCNPs reduced significantly; hence, the cell viability after exposition to UCNPs-NH_2-FA resulted to be more than 80% for all the tested concentrations. This confirms that functionalized UCNPs-NH_2-FA showed no affection on the metabolic state of the three cancer cells here studied: HeLa and breast cancer cells MD-MB-231 and MCF7. This result is a desirable feature for biolabels tools, because this assures that they can bind to their cancer cell target, without damage it or any other cells located in the surrounding area of the tumor.

There is an increased concern related to hazards of nanomaterials in biological systems, especially those applied in biomedicine and food. In nanotoxicology, besides cytotoxicity assays it is also important to measure the genotoxicity effects of the tested nanomaterial. This can be achieved by several strategies including comet and micronucleus assays. It has been reported that there is a strong consistency between the genotoxicity effects of a nanoparticle measured by the comet assay with those obtained by the micronucleus assay [35]. Although the bioaccumulation of UCNPs in mice has been reported [36], to our knowledge there have not been reports of their genotoxic effects. Therefore, we decided to evaluate the genotoxicity of both bare UCNPs and functionalized UCNPs-NH_2-FA by comet assay in HeLa, MDA-MB-231 and MCF7 cancer cells treated with different concentrations of UCNPs. The results revealed that none of concentrations of both bare and functionalized UCNPs herein tested provokes DNA damage in treated cells. Hence, with the MTT and comet assays, it was possible to determine that all the concentrations herein used of both bare and functionalized UCNPs resulted to be no cytotoxic and no genotoxic.

Numerous studies have reported the application of UCNPs for in vitro cellular imaging [32]. In vitro cellular imaging involves targeting of UCNPs to some subcellular components, such as FA receptor [37–39]. The advantage of UCNPs over their respective lanthanide bulk material is that the former are photoexcitable in the NIR spectra, for example, at 980 nm such as the UCNPs of $Y_2O_3/Er^{3+}/Yb^{3+}$ (1, 1%) here studied. At this wavelength, the auto-absorption of any biological sample is weak, reducing with this the absorption and luminescence background [27].

It is known that some cancer cells express FR in their cell membrane, facilitating with this the uptake of any ligand bound to this FR [40]. This was our reasoning to functionalize UCNPs with FA to promote the internalization of UCNPs-NH_2-FA into cancer cells. To confirm this, we incubated the UCNPs-NH_2-FA with cervical adenocarcinoma HeLa cells and breast cancer cells lines MDA-MB-231 and MCF7, to evaluate if the UCNPs-NH_2-FA were able to bind to FA receptor expressed on their cell membrane and been uptaken by the cells. We showed that the luminescence of UCNPs-NH_2-FA emission at 554 nm was detectable using confocal microscopy. Moreover, it was demonstrated that UCNPs-NH_2-FA were able not only to bind but also to internalize into the cytoplasm of the HeLa, MDA-MB-231 and MCF7 cancer cells. With these, we demonstrate that UCNPs-NH_2-FA here synthetized are able not only to bind but to be uptaken by cancer cells that overexpress FA receptors on their cell membrane.

In attempts to use this UCNPs-NH2-FA as cancer cell biolabels for diagnosis, it is important to test an efficient and rapid method for cancer cell detection. For this, we took advantage of the intrinsic green fluorescence of UCNPs to test whether their binding

to cancer cell lines could be detected by a conventional method used in diagnosis such as flow cytometry. Moreover, since the internalization of UCNPs-NH2-FA was previously demonstrated, we decided that UCNPs-NH2-FA binding and uptake could be measure by flow cytometry. Indeed, the obtained results demonstrated that only UCNPs-NH2-FA bound to cervical adenocarcinoma (HeLa) cells and breast cancer cells (MDA-MB-231 and MCF7), while bare UCNPs were not able to bind to these cells and no detection was observed.

Thus, the results of biological experiments are supported by a complete physicochemical characterization of the UCNPs here used. Indeed, we also present the assessments for nanotoxicology evaluation of UCNPs. It is possible to use these UCNPs-NH2-FA as biolabels for cancer cells, since it was possible to visualize and detect them by confocal microscopy and flow cytometry. It is important to mention that due to their lack of both cytotoxicity and genotoxicity and no fading of color, UCNPs can be used for a longer period of time is the energy source is maintained, especially in for diagnosis imaging to have an efficiently contrast agent for better imaging, diagnosis and therapy. The inorganic UCNPs have unique optical properties that can have a potential for wide applications such as magnetic resonance imaging (MRI), ultrasonography, optical imaging devices and positron emission tomography (PET) [41]. Moreover, their excitation wavelength at NIR light corresponds to the optical biological window that avoids the photodamaging of cells but allows a deep penetration in tissue cells. So, this study paves the way to further testing the usage of this type of UCNPs-NH2-FA for in vivo studies in animal models of cancer as detection nanoprobes.

Conclusions

In this study, we demonstrate that UCNPs Y_2O_3; Er^{3+}, Yb^{3+} (1, 1 mol%) covered with silica and functionalized with folic (UCNPs-NH_2-FA) showed intense green emission spectra at 554 nm, under near-infrared excitation at 980 nm. Also we confirm that UCNPs-NH_2-FA exhibit an excellent biocompatibility because their cytotoxicity was null after being functionalized and no genotoxicity and DNA damage was detected by their incubation with cancer cells.

Moreover, UCNPs-NH_2-FA were intracellular visualized in cervix adenocarcinoma HeLa cells and MCF7 and MB-MDA-231 breast cancer cells, and also it was possible to confirm their cell binding by flow cytometry by detecting UCNPs-NH_2-FA green emission. This confirms their purpose as cancer cell biolabels. These functionalized UCNPs-NH_2-FA represent an advanced diagnosis tool based on nanotechnology for applications as biolabels for in vivo murine models of breast and cervical cancer and open the door to be considered as cancer diagnosis nanotools.

Acknowledgements

The authors wish to acknowledge financial support from DGAPA-UNAM Grant No. 109913 and CONACYT Project No. 269071. DGAPA-UNAM Grant No. 111017 and CONACYT Project Nos. 269071 and 232608. The authors acknowledge the technical support provided by E. Aparicio, F. Ruiz. M. Ponce, Dr. Katrin Quester, Dr. F. Castillón and Dr. Ruben D. Cadena Nava. The authors are grateful with the facilities provided by Dr. Rosa Mouriño at the Centro de Microscopía Avanzada (CEMIAD) of CICESE in the use of confocal microscopy and Dr. Olga Callejas for her technical assistance in imaging capture. Karla Juarez-Moreno is a member of the International Network of Bionanotechnology with impact in Biomedicine, Food and Biosafety (Funded by CONACYT Project 279889).

Compliance with ethical standards

Conflicts of interest The authors declare that they have no conflicts of interest.

Electronic supplementary material: The online version of this article (https://doi.org/10.1007/s10853-017-1946-0) contains supplementary material, which is available to authorized users.

References

[1] Lin M, Zhao Y, Wang S et al (2012) Recent advances in synthesis and surface modification of lanthanide-doped upconversion nanoparticles for biomedical applications.

Biotechnol Adv 30:1551–1561. https://doi.org/10.1016/j.biotechadv.2012.04.009

[2] Wang M, Abbineni G, Clevenger A et al (2011) Upconversion nanoparticles: synthesis, surface modification and biological applications. Nanomed Nanotechnol Biol Med 7:710–729. https://doi.org/10.1016/j.nano.2011.02.013

[3] Matsuura D (2002) Red, green, and blue upconversion luminescence of trivalent-rare-earth ion-doped Y_2O_3 nanocrystals. Appl Phys Lett 81:4526. https://doi.org/10.1063/1.1527976

[4] Yang Y (2014) Upconversion nanophosphors for use in bioimaging, therapy, drug delivery and bioassays. Microchim, Acta

[5] Shen J, Sun L-D, Yan C-H (2008) Luminescent rare earth nanomaterials for bioprobe applications. Dalt Trans. https://doi.org/10.1039/b805306e

[6] Blasse G, Grabmaier B (1994) Luminescent materials, 1st edn. Springer, Berlin

[7] Chen GY, Liu Y, Zhang ZG et al (2007) Four-photon upconversion induced by infrared diode laser excitation in rare-earth-ion-doped Y_2O_3 nanocrystals. Chem Phys Lett 448:127–131. https://doi.org/10.1016/j.cplett.2007.09.078

[8] Kong W, Shan J, Ju Y (2010) Flame synthesis and effects of host materials on Yb^{3+}/Er^{3+} co-doped upconversion nanophosphors. Mater Lett. https://doi.org/10.1016/j.matlet.2009.12.039

[9] Sounderya N, Zhang Y (2009) Upconversion nanoparticles for imaging cells. In: IFMBE proceedings, pp 1741–1744

[10] Anderson RR, Parrish JA (1981) The optics of human skin. J Invest Dermatol 77:13–19. https://doi.org/10.1016/j.artres.2008.11.002

[11] Wang C, Tao H, Cheng L, Liu Z (2011) Near-infrared light induced in vivo photodynamic therapy of cancer based on upconversion nanoparticles. Biomaterials 32:6145–6154. https://doi.org/10.1016/j.biomaterials.2011.05.007

[12] Alexis F, Rhee J-WW, Richie JP et al (2008) New frontiers in nanotechnology for cancer treatment. Urol Oncol Semin Orig Investig 26:74–85. https://doi.org/10.1016/j.urolonc.2007.03.017

[13] Sudimack J, Lee RJ (2000) Targeted drug delivery via the folate receptor. Adv Drug Deliv Rev 41:147–162. https://doi.org/10.1016/S0169-409X(99)00062-9

[14] Lu Y, Sega E, Leamon CP, Low PS (2004) Folate receptor-targeted immunotherapy of cancer: mechanism and therapeutic potential. Adv Drug Deliv Rev 56:1161–1176. https://doi.org/10.1016/j.addr.2004.01.009

[15] Yee K, Seow E, Zhang Y, Chyn Y (2013) Biomaterials targeting CCL21 e folic acid e upconversion nanoparticles conjugates to folate receptor-a expressing tumor cells in an endothelial-tumor cell bilayer model. Biomaterials 34:4860–4871. https://doi.org/10.1016/j.biomaterials.2013.03.029

[16] Rijnboutt S, Jansen G, Posthuma G et al (1996) Endocytosis of GPI-linked membrane folate receptor-alpha. J Cell Biol 132:35–47. https://doi.org/10.1083/jcb.132.1.35

[17] Wu M, Gunning W, Ratnam M (1999) Expression of folate receptor type alpha in relation to cell type, malignancy, and differentiation in ovary, uterus, and cervix. Cancer Epidemiol Biomark Prev 8:775–782

[18] Taxak VB, Khatkar SP, Han S-D et al (2009) Tartaric acid-assisted sol–gel synthesis of Y_2O_3:Eu^{3+} nanoparticles. J Alloys Compd 469:224–228. https://doi.org/10.1016/j.jallcom.2008.01.088

[19] Chávez DH, Contreras OE, Hirata GA (2016) Synthesis and upconversion luminescence of nanoparticles Y_2O_3 and Gd_2O_3 Co-doped with Yb^{3+} and Er^{3+}. Nanomater Nanotechnol. https://doi.org/10.5772/62188

[20] Stöber W, Fink A, Bohn E (1968) Controlled growth of monodisperse silica spheres in the micron size range. J Colloid Interface Sci 26:62–69. https://doi.org/10.1016/0021-9797(68)90272-5

[21] Chavez DH, Juarez-Moreno K, Hirata GA (2016) Aminosilane functionalization and cytotoxicity effects of upconversion nanoparticles Y_2O_3 and Gd_2O_3 co-doped with Yb^{3+} and Er^{3+}. Nanobiomedicine. https://doi.org/10.5772/62252

[22] De Mello JC, Wittmann HF, Friend RH (1997) An improved experimental determination of external photoluminescence quantum efficiency. Adv Mater 9:230–232. https://doi.org/10.1002/adma.19970090308

[23] Mosmann T (1983) Rapid colorimetric assay for cellular growth and survival: application to proliferation and cytotoxicity assays. J Immunol Methods 65:55–63

[24] Singh NP, McCoy MT, Tice RR, Schneider EL (1988) A simple technique for quantitation of low levels of DNA damage in individual cells. Exp Cell Res 175:184–191

[25] Speit G, Hartmann A (2006) The comet assay: a sensitive genotoxicity test for the detection of DNA damage and repair. Methods Mol Biol 314:275–286. https://doi.org/10.1385/1-59259-973-7:275

[26] Sánchez-Sánchez L, Tapia-Moreno A, Juarez-Moreno K et al (2015) Design of a VLP-nanovehicle for CYP450 enzymatic activity delivery. J Nanobiotechnol 13:1–10. https://doi.org/10.1186/s12951-015-0127-z

[27] Mader HS, Kele P, Saleh SM, Wolfbeis OS (2010) Upconverting luminescent nanoparticles for use in bioconjugation and bioimaging. Curr Opin Chem Biol 14:582–596. https://doi.org/10.1016/j.cbpa.2010.08.014

[28] Wang M, Mi C, Zhang Y et al (2009) NIR-responsive silica-coated NaYbF 4:Er/Tm/Ho upconversion fluorescent

nanoparticles with tunable emission colors and their applications in immunolabeling and fluorescent imaging of cancer cells. J Phys Chem C 113:19021–19027. https://doi.org/10.1021/jp906394z

[29] Chatterjee DK, Rufaihah AJ, Zhang Y (2008) Upconversion fluorescence imaging of cells and small animals using lanthanide doped nanocrystals. Biomaterials 29:937–943. https://doi.org/10.1016/j.biomaterials.2007.10.051

[30] Chen G, Qiu H, Prasad PN, Chen X (2014) Upconversion nanoparticles: design, nanochemistry, and applications in theranostics. Chem Rev 114:5161–5214. https://doi.org/10.1021/cr400425h

[31] Low PS, Henne WA, Doorneweerd DD (2008) Discovery and development of folic-acid-based receptor targeting for imaging and therapy of cancer and inflammatory diseases. Acc Chem Res 41:120–129. https://doi.org/10.1021/ar7000815

[32] Ai J, Xu Y, Li D et al (2012) Folic acid as delivery vehicles: targeting folate conjugated fluorescent nanoparticles to tumors imaging. Talanta 101:32–37. https://doi.org/10.1016/j.talanta.2012.07.075

[33] Davis ME, Chen ZG, Shin DM (2008) Nanoparticle therapeutics: an emerging treatment modality for cancer. Nat Rev Drug Discov 7:771–782. https://doi.org/10.1038/nrd2614

[34] Yoon SN, Ku J-L, Shin Y-K et al (2007) Hereditary non-polyposis colorectal cancer in endometrial cancer patients. Int J Cancer 122:1077–1081. https://doi.org/10.1002/ijc.22986

[35] Karlsson HL, Di Bucchianico S, Collins AR, Dusinska M (2015) Can the comet assay be used reliably to detect nanoparticle-induced genotoxicity? Environ Mol Mutagen 56:82–96. https://doi.org/10.1002/em.21933

[36] Cheng L, Yang K, Shao M et al (2011) In vivo pharmacokinetics, long-term biodistribution and toxicology study of functionalized upconversion nanoparticles in mice. Nanomedicine 6(8):1327–1340. https://doi.org/10.2217/nnm.11.56

[37] Shen J, Zhao L, Han G (2013) Lanthanide-doped upconverting luminescent nanoparticle platforms for optical imaging-guided drug delivery and therapy. Adv Drug Deliv Rev 65:744–755. https://doi.org/10.1016/j.addr.2012.05.007

[38] Hemmer E, Yamano T, Kishimoto H et al (2013) Cytotoxic aspects of gadolinium oxide nanostructures for up-conversion and NIR bioimaging. Acta Biomater 9:4734–4743. https://doi.org/10.1016/j.actbio.2012.08.045

[39] Cheng L, Yang K, Li Y et al (2011) Facile preparation of multifunctional upconversion nanoprobes for multimodal imaging and dual-targeted photothermal therapy. Angew Chemie 123:7523–7528. https://doi.org/10.1002/ange.201101447

[40] Subik K, Lee J-F, Baxter L et al (2010) The expression patterns of ER, PR, HER2, CK5/6, EGFR, Ki-67 and AR by immunohistochemical analysis in breast cancer cell lines. Breast Cancer (Auckl) 4:35–41

[41] Qian J, Wang D, Cai F et al (2012) Photosensitizer encapsulated organically modified silica nanoparticles for direct two-photon photodynamic therapy and in vivo functional imaging. Biomaterials 33:4851–4860. https://doi.org/10.1016/j.biomaterials.2012.02.053